IMPERIAL

Simulation-guided Suspension Design for a Motor Vehicle

Individual Project Report

ME4 Individual Project

11/06/2026

Imperial College London

Department of Mechanical Engineering

Author: Michael Suli

Supervisor: Alexis B. Ihracska

Pages: 28

Words: 7596

Abstract

Whether designing a race car or luxury vehicle, vehicle suspension provides the sole link between the tyre contact patch, where all forces are transmitted to the road to generate grip, and the chassis. Managing the way forces are transmitted from the chassis to the tyres, via the suspension, enables designers to achieve performance targets and innovate on previous designs. This project aims to provide designers with the simulation tools necessary to iterate suspension design, reduce costs associated with using industry standard software and relate suspension design directly to on track performance. The context of a Formula Student car was used throughout this project, as it will enable the Imperial Formula Racing (IFR) team to build understanding of suspension design using tools without resorting to expensive external software.

A kinematic design analysis tool was created in MATLAB to analyse parametric effects of bump (vertical movement), roll (rotation due to cornering) and steering. The parametric analysis was validated against Applied Racing Dynamics (ARD), used by the IFR team, where validation is critical to inspiring confidence in the outputs for design use. A 31.8% maximum RMS error is found and is diagnosed as a difference in contact patch calculation between the in-house tool and ARD.

Subsequently, a Quasi-Static Lap Simulation tool was created to evaluate the effectiveness of suspension kinematic changes. The tool was validated against both ARD and IFR telemetry, to provide a tool that could confidently predict lap time improvements. When both tools were applied to the IFR use case, a lap time reduction of 1.45s was realised, worth 4 places at the FSUK2025 sprint event. The development of these tools will enable the IFR team to transition to a yearly development cycle, with detailed suspension and vehicle dynamics analysis to support design decisions.

Acknowledgements

I would like to thank my supervisor, Alexis B. Ihracska, for taking on this self-proposed project. His support and guidance throughout has allowed this project to reach its full potential.

Additional thanks are given to the Imperial Formula Racing (IFR) team, of which I am a proud member, for providing access to data and resources which were critical to the completion of this project.

Table of Contents

1. Introduction

A vehicle's suspension is the sole link between the chassis and the tyre, where the only connection to the road surface occurs and grip is generated. The generation of grip is influenced by the parameters experienced at the contact patch, such as camber, which can lead to different grip values, thus managing these parameters through suspension design can yield significant performance benefits for a motor vehicle. The purpose of suspension design is to maintain the tyre at the optimum angle to the road surface in all conditions [1].

Design of suspension is hampered by scarcity of literature and the expense of industry-standard software packages. Suspension design documentation is closely guarded as suspension is a key performance differentiator between competitors in the motor industry and motorsports.

The Imperial Formula Racing (IFR) team finds itself spending a significant proportion of its limited budget on industry-standard software, which otherwise would be used for car development as they seek to move to a yearly development cycle.

The objectives of this project are:

- Review existing kinematic analysis and lap simulation tools, such as Applied Racing Dynamics.
- Develop analysis tools capable of providing parametric suspension analysis.
- Validate tools against industry standard software.
- Apply developed tools in the design of the IFR02 front suspension.

2. Literature Review

The design of suspension componentry in motor vehicles has evolved since the inception of the motor vehicle. This review and project will focus on the double wishbone suspension type, following on from a previous literature review 'Single Seater Race Car Optimisation' [2].

2.1. Double Wishbone Suspension

A double wishbone suspension (DWS) is used primarily on high performance and heavy-duty vehicles [3]. DWS consists of two 'A-arms' which connect the wheel to the chassis and are chosen because of their ability to tune handling of suspension parameters through manipulation of geometry and optimisation to achieve the handling targets set out in a design brief [1].

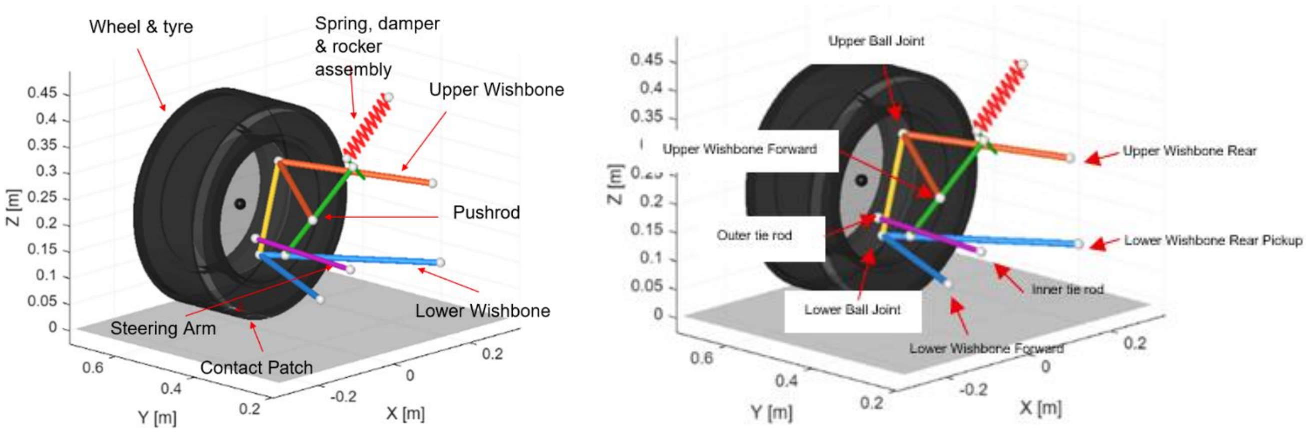

Figure 1: Double Wishbone Suspension Annotated a) Components, b) Hardpoints

The double wishbone suspension example in Figure 1 illustrates the arrangement of a typical pushrod actuated front suspension system, adjusting the locations of hardpoints will affect multiple parameters simultaneously.

2.2. Suspension Parameters and Movement

There are three primary types of suspension movement which influence its kinematics: bump/rebound (vertical displacement of the wheel), roll (chassis rotation about the x-axis) and steering (wheel rotation through the tie rod)[1].

Applying any single one of these movements to the suspension system will cause suspension parameters, such as camber gain, bump steer or roll centre height, to vary. The primary role of a suspension system is to maintain optimal angle of the wheels to the road at any given time [4] and is achieved through manipulation of suspension kinematics to optimise these parameters through the design of pickup points to optimise tyre usage.

Camber is the inclination of the wheel when viewed from the front-view, with negative camber achieved when the wheel leans inwards, Figure 2. It is a critical parameter in ensuring the tyres experience the optimal contact patch, particularly during cornering where roll effects can lead to positive camber and adverse handling [4].

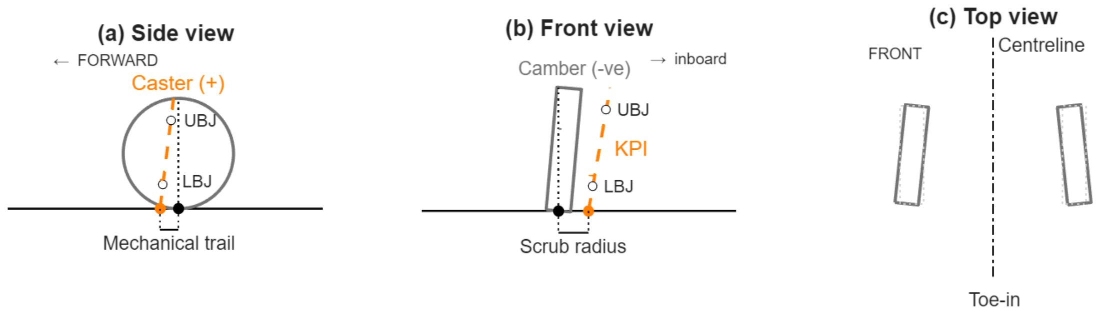

Figure 2: Illustration of suspension parameters in side, front and top view

Caster is the inclination angle between the upper and lower ball joint in the side-view and provides a self-centring effect for the steering system. When caster is projected to the ground, the distance to the contact patch provides the self-centring effect called mechanical trail.

Kingpin inclination (KPI) is the angle between the upper and lower ball joint in the front-view and forms the steering axis of the car. The distance between the KPI projection to the ground and the contact patch gives the scrub radius, providing the steering effort effect and vehicle stability.

Table 1 : Recommended range of suspension values [5]

Parameter:	Maximum Value:	Minimum Value:
KPI (deg)	6	0
Scrub Radius (mm)	30	12
Mechanical Trail (mm)	30	12
Caster Angle (deg)	10	4
Camber Angle (deg)	3	0
Toe Angle (deg)	3	0

Toe is the angle of the wheel to the centre line from the top-view. Toe-in is when the tyres point towards the centreline, promoting straight line stability and toe-out when they point outwards, promoting better turn in. Bump steer is an issue that causes an individual wheel's toe to vary over bumps, causing instability as the car steers in the toe direction.

Instant centres (IC) are formed at the intersection of the wishbone arm projections, Figure 3, then the roll centre is found by projecting the IC to the contact patch. The roll centre influences lateral load transfer transmission and should always be above the ground.

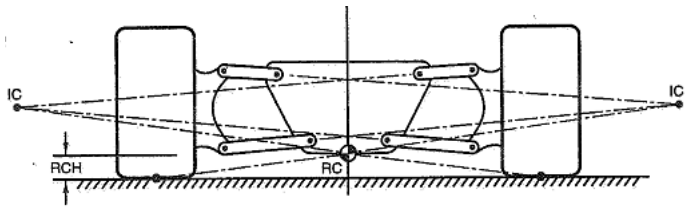

Figure 3: Instant centre and roll centre formulation [4]

Table 1 shows the typical range of suspension parameters for a Formula Student car and provides a baseline for suspension design.

2.3. Suspension Optimisation Process and Software Choice

The suspension optimisation process involves setting performance targets, whether kinematic or lap time based, and adjusting hardpoints to find the correct compromise between parameters [2].

There are two schools of thought when optimising suspension geometry, manual iteration and automated optimisation. Manual iteration involves the designer adjusting hardpoints to achieve the desired parameters, whilst automated optimisation sets boxes for hardpoint locations, utilising an algorithm to solve to achieve desired parametric targets. The manual process is much more time consuming but has significantly lower computational expense, not requiring an extensive optimisation algorithm and effort to ensure refinement of output.

Various suspension simulation tools are available, such as ADAMS, Applied Racing Dynamics (ARD) and OptimumK, which require a steep learning curve, high licensing fees (£1000 for OptimumK optimisation) and use limits. ARD exists as a manual iteration package, whilst OptimumK has functionality for both options. The two packages also offer lap simulation capabilities to test the lap time improvement of suspension design iteration [3]. Manual iteration is typically preferred in FS as it enables knowledge build up in the design process for amateur motorsport engineers and can be cited in each team's design presentation. The IFR team currently utilises the ARD package to simulate vehicle dynamics and conduct suspension analysis, with this software being the baseline for validation of the tools generated in this report.

To create the tools required in this project, a software base was required that could compute multibody dynamics whilst remaining accessible to university students. Dymola and MATLAB were considered, with MATLAB ultimately being chosen because it is readily available without having to pay for a license. MATLAB is matrix based and can solve numerically complex problems with multiple degrees of freedom as is required in this project.

2.4. Vehicle Dynamics and Lap Simulation Analysis

Lap simulations provide analysis of vehicle properties over a lap to ascertain the performance of a vehicle and are important in quantifying performance improvement of design changes. Three simulation types exist: point-mass, quasi-static and dynamic [6].

Point mass simulations (PMS) model vehicles as a single lumped mass where performance in cornering, acceleration and braking is governed by a friction circle. PMS are quick and simple to model but lack fidelity as they don't represent load transfer or individual tyre loads.

Quasi-static lap simulations (QSLS) are most utilised for their ability to capture vehicle dynamics effects such as load transfer and grip without utilising excessive computational power. A QSLS evaluates static equilibrium at each discrete point around a lap, providing the maximum possible acceleration at each point to evaluate vehicle performance [7].

Dynamic lap simulations are much more computationally taxing as they evaluate all dynamics events that the car experiences throughout its operation, including damper effects and yaw dynamics [6]. Whilst the highest fidelity, it is the most computationally taxing and is outside of the scope of this project.

2.4.1. QSLS Formation

QSLS utilise a forward and backward pass to compute the maximum acceleration and deceleration between two given points to give the speed profile. They vary in complexity with fidelity depending on the concepts utilised, such as load transfer, spring rates and the tyre model used [8]. Acceleration is limited by available engine power and available grip for both passes, with the lateral grip demand prioritised to give the lateral acceleration and remaining grip force used for longitudinal acceleration.

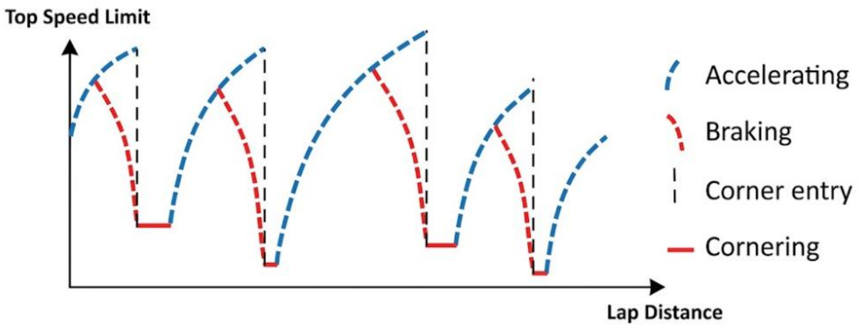

Figure 4: Forward and backward passes generating speed profile [12]

Reconciling the speed between each discretisation in the track is achieved using:

$$v^2 = u^2 + 2as$$

Where v is the instant speed, u is the previous speed, a is the acceleration and s is the distance between the two points.

To ensure the car remains within its performance envelope throughout the lap, the final speed profile is taken as the minimum of the forward and backward pass at each point [6], where the forward pass governs corner exits and straights whilst the backward pass governs braking as seen in Figure 4.

2.4.2. Vehicle Dynamics Concepts

This section establishes some of the key vehicle dynamics concepts which add fidelity to the lap simulation, by varying tyre vertical load and chassis roll [4].

Wheel rate is the vertical stiffness at the contact patch and is used to relate the spring stiffness to what is experienced at the tyre and is given by:

$$K_w = K_s(MR)^2$$

Where K_w is the wheel rate, K_s is the spring rate and MR is the suspension motion ratio. The Motion Ratio is utilised to manipulate the wheel rate of the car with pushrod rocker geometry:

$$MR = \frac{Wheel\ Displacement}{Damper\ Displacement}$$

Roll stiffness is the resistance to the roll moment:

$$K_{roll} = \frac{1}{2}K_w t^2$$

Where K_{roll} is the roll stiffness, K_w is wheel rate and t is the track width.

The roll moment is created in cornering, and causes the chassis to roll about the roll axis:

$$M_{roll} = m \cdot a_y(h_{CoG} - h_{rc})$$

Where M_{roll} is roll moment, m is vehicle mass, a_y is the lateral acceleration, h_{CoG} is the centre of gravity height and h_{rc} is roll centre height. Lateral load transfer is the redistribution of vertical load due to lateral acceleration in cornering. LLT is split into two components, geometric and elastic. The geometric component transfers load directly through suspension links:

$$\Delta F_{z,geo} = \left(m \cdot a_y \cdot \frac{b}{L}\right) \cdot \frac{h_{rc}}{t}$$

Where m is vehicle mass, a_y is the lateral acceleration, b is the distance between the CoG and rear axle, L is the wheelbase. Elastic load transfer is reacted through the springs rather than the suspension links, given by:

$$\Delta F_{z,elastic} = \left(\frac{K_{roll,axle}}{K_{roll,total}}\right) * \frac{M_{roll}}{t}$$

Longitudinal load transfer is the equivalent to lateral load transfer for braking or acceleration:

$$\Delta F_{z,lon} = m \cdot a_x \cdot \frac{h_{CoG}}{L}$$

Where a_x is longitudinal acceleration.

2.5. Lap Performance Analysis

Two common vehicle performance metrics are commonly used, shown in Figure 5.

Firstly, a speed-distance trace is utilised as differences in speeds between two traces indicates a time and performance difference. The peaks in a speed-distance trace indicate straights, whilst the troughs are the cornering potential.

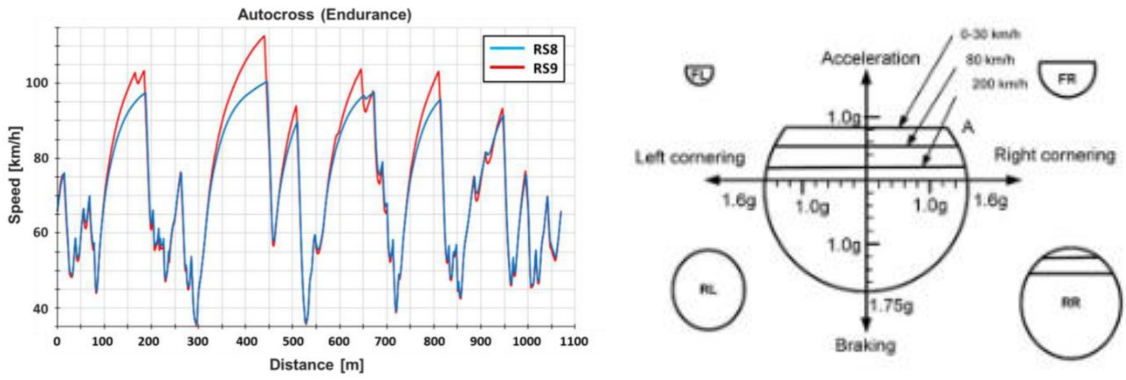

Figure 5: Lap analysis plots a) speed-distance trace [13], b) g-g diagram [1]

Secondly, a g-g plot is used to illustrate the instantaneous lateral and longitudinal acceleration at each point in a lap. Wider g-g envelopes indicate improved cornering performance, whilst taller g-g diagrams indicate better acceleration out of corners and braking.

2.6. Tyre model

A tyre model is key for interpreting vehicle performance through analysis of how a car utilises its tyres. No two tyres give the same force for a given set of operating conditions and are characteristically non-linear in their outputs [1].

Slip angle is the difference between the tyre heading and the direction the contact patch travels. Peak grip is not generated at the same vertical force or slip angle, hence managing slip angles is key to generating the optimal grip in cornering.

The IFR tyre model is constructed by analysis of Tyre Testing Consortium (TTC) data for the chosen IFR02 tyre, determining Pacejka coefficients and using these coefficients to construct the necessary tyre data [9]. The resulting tyre model is shown in Figure 6 and is utilised in the code through a lookup table with vertical force, camber and slip angle, with analysis from the IFR team indicating a peak-grip camber of -0.4°.

Figure 6 shows the non-linearity of the tyre model, where lateral force varies with applied vertical load and slip angle, saturating at higher loads. The lateral force indicates the available grip for

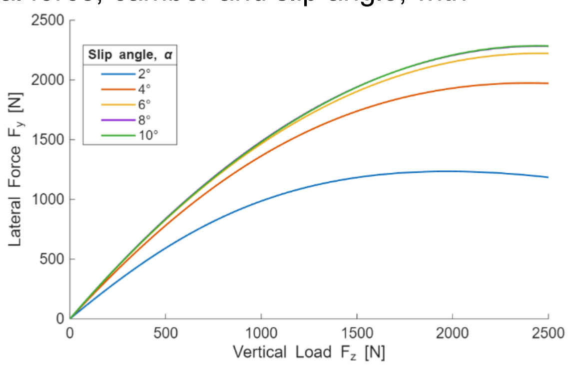

Figure 6: Lateral force vs vertical load for given slip angles

cornering, hence this load and slip sensitivity directly impacts vehicle cornering performance. To account for wet weather conditions, a grip scaling factor of 0.55-0.70 is applied to reduce the ability for tyres to generate their maximum grip [10].

3. Kinematic Analysis

3.1. Purpose of the Tool

The purpose of the kinematic analysis tool is to analyse and visualise suspension throughout the development process over the various suspension movements: bump, steer and chassis roll. Suspension geometry is parameterised using hardpoint coordinates, utilising constant length and rigid link constraints to resolve suspension motion and enable analysis.

Understanding of how kinematic parameters, such as camber gain, bump steer and roll centre height, impact performance means designers can set targets in design to promote rapid development of geometric hardpoints to achieve said targets.

Initially, a 2D kinematic analysis tool was created, providing visualisation and analysis with lower computational effort. A 2D model provides the opportunity for inexperienced suspension designers to learn how varying hardpoints will lead to kinematic difference, whilst reducing complexity by omitting 3D parameters such as caster, toe and scrub radius.

Subsequently, a 3D analysis tool was developed to improve kinematic analysis through the inclusion of 3D parameters such as caster, toe and scrub radius. Here, the methods developed for the 2D analysis were extended to 3D to simplify the process and enabled focus on developing analysis for bump, roll and steer analysis, as well as creating the functionality for combined analysis.

3.2. Methods

This section outlines the developmental approach used to develop the kinematic analysis tool in MATLAB, progressing from 2D to 3D analysis for analysis of bump, roll and steer movement.

3.2.1. Mathematical Formulation & Implementation

To enable consistent, reliable kinematic analysis of a double wishbone suspension, a robust method for prescribing movement and maintaining accuracy was required. Here, the suspension arms and chassis hardpoints are constrained by rigid fixed lengths, using a residuals method, so that suspension motion can be solved as a constrained multibody problem.

The Levenberg-Marquardt algorithm is utilised to resolve the residuals of link-length through suspension movement to be close to zero and maintain geometric continuity throughout.

To ensure the solver function reaches the correct values, the correct number of degrees of freedom, boundary conditions and initial guesses were defined carefully to prevent solver failure or flipping over incremental suspension movements whilst maintaining accuracy of solver output.

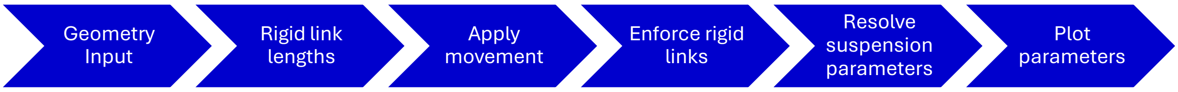

Figure 7: Kinematic analysis tool solver workflow

For bump motion, Figure 8, the wheel centre (WC) height is varied and passes through the solver functions and residual driver which then resolves the prescribed motion in the z-direction whilst the chassis hardpoints remain rigidly fixed in place.

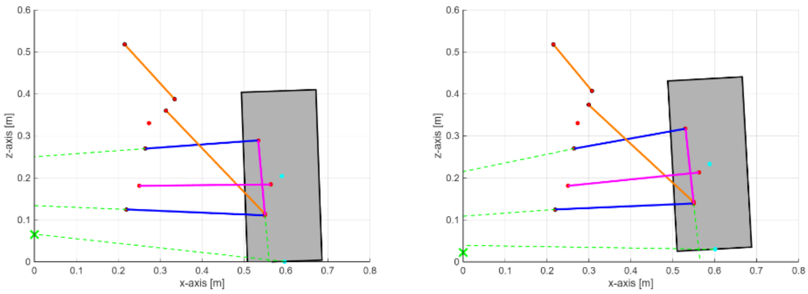

Figure 8: Front-view suspension in bump a) 0mm bump travel, b)30mm bump travel

For roll motion, Figure 9, the chassis hardpoints are rotated about the Centre of Gravity whilst the remainder of the suspension is articulated because of this suspension motion.

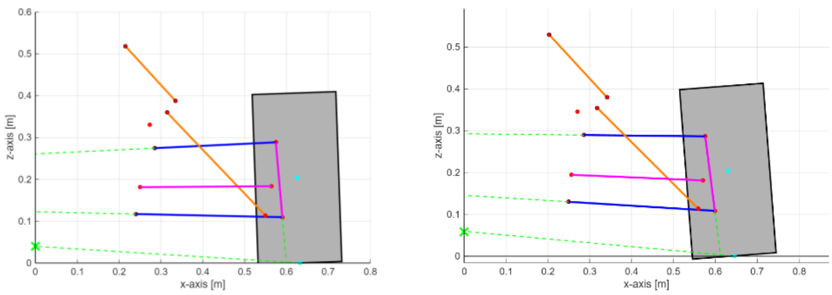

Figure 9: Front-view suspension in roll a) 0° roll, b) 3° roll

For steer motion, Figure 10, the track rod (steering arm) is translated in the y-axis in the same way that a regular steering rack would do. Here, no other movement is specified to the remainder of the suspension system and the suspension kinematics are influenced solely by the motion of the track rod.

At each incremental step, suspension parameters are calculated from the resulting WC, CP and hardpoint locations and stored in the script, to be plotted for analysis.

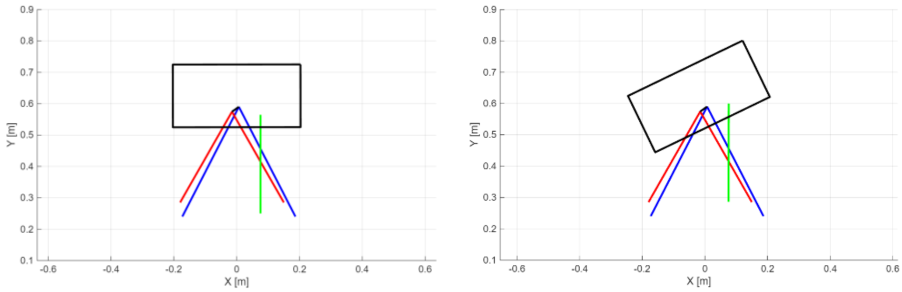

Figure 10: Top-view suspension in steer a) 0mm steering travel, b) 36mm steering travel

3.2.2. Assumptions and Limitations

The primary assumption is the suspension members obey rigid body motion, whereby arms and links don't flex, whilst, in reality, suspension arms will inevitably deflect in motion and influence the suspension kinematics. This is termed suspension compliance and can be detrimental to suspension kinematic performance. Tyre compliance is not modelled, as the tyres are considered infinitely stiff, whilst reality dictates that tyres have a finite stiffness, on average 10x that of a typical coil spring [2].

A further simplification is made in roll analysis, where the CoG height position is used at the car centreline as opposed to the instantaneous roll centre position at each previous step. This was chosen as the roll centre migrates location throughout suspension movement, as would often lead to the solver failing and hence analysis not being computed.

3.3. Results

3.3.1. Validation against ARD

In this section, results of kinematic analysis are analysed against Applied Racing Dynamics (ARD). A Root-Mean-Square analysis of the inhouse kinematic tool compared to the IFR's chosen vehicle dynamics package was undertaken. An RMS analysis was used because of its ability to provide a quantitative value for the error against a baseline and penalise large discrepancies which impact the accuracy of the tool compared to the ARD baseline.

3.3.1.1. Bump Analysis

Figure 11 depicts the RMS errors obtained in the comparison of suspension parameters in ±30mm of bump travel.

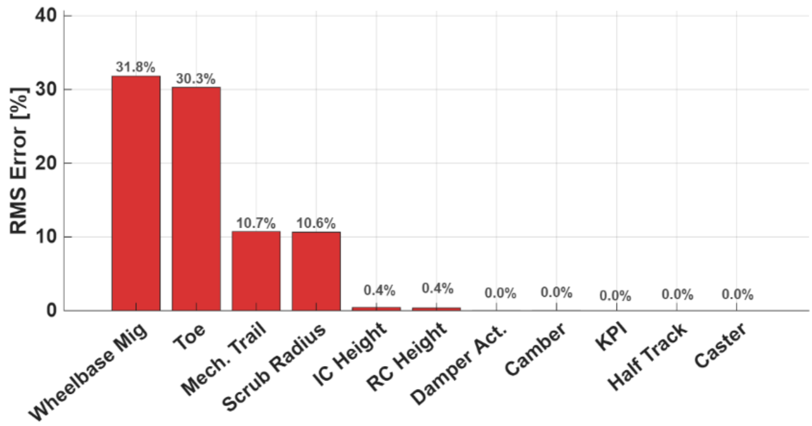

Figure 11: RMS errors for suspension parameters in bump

Figure 12 provides an overlay of two outputs of bump analysis in ARD compared to the in-house solver. In Figure 12b, a 31.8% RMS error in wheelbase migration is obtained, whilst in Figure 12a a zero RMS error in camber is obtained.

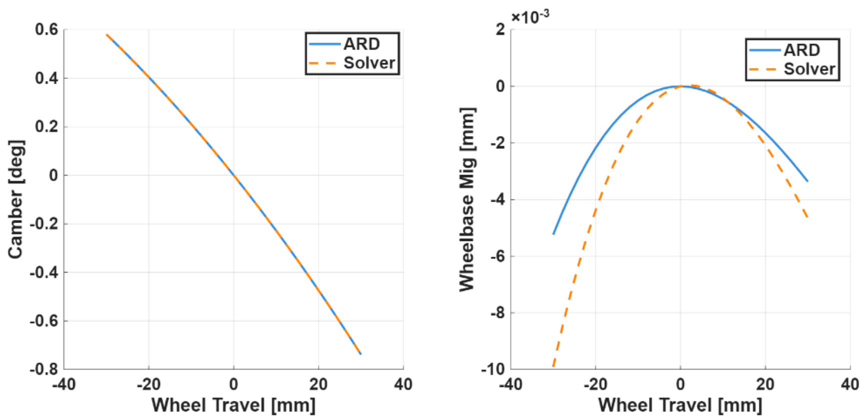

Figure 12: Kinematic solver vs ARD comparison in bump for a) camber, b) wheelbase migration

3.3.1.2. Roll Analysis

Figure 13 illustrates the RMS errors obtained for suspension parameters in ±3 degrees of roll.

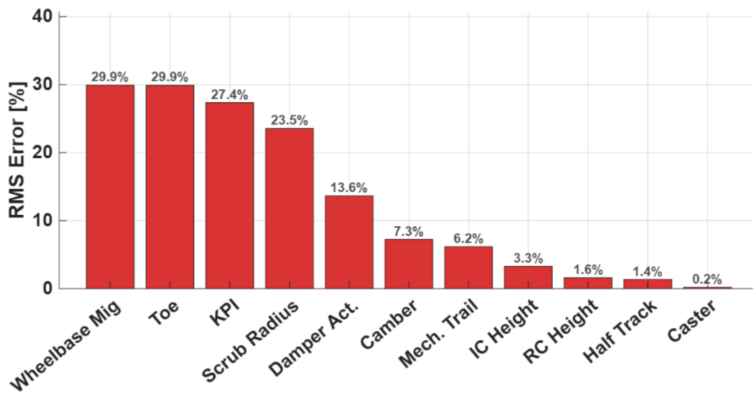

Figure 13: RMS errors for suspension parameters in roll

Figure 14 provides an overlay of two different outputs in both ARD and kinematic tool with different RMS values to illustrate how the differences appear physically. In Figure 14a, wheelbase migration is shown, leading to an RMS error of 29.9% whilst Figure 14b shows roll centre height which led to an RMS error of 1.6%.

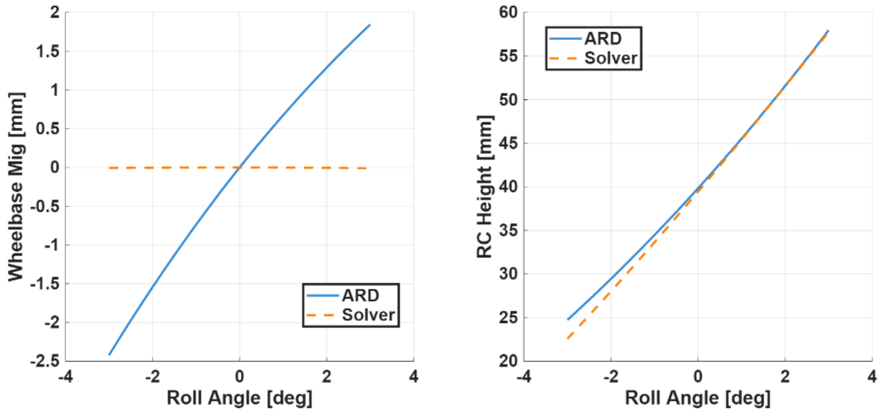

Figure 14: Kinematic solver vs ARD comparison in roll for a) wheelbase migration b) roll centre

3.3.1.3. Steer Analysis

Figure 15 illustrates the RMS error of each individual suspension parameter with ARD as the baseline.

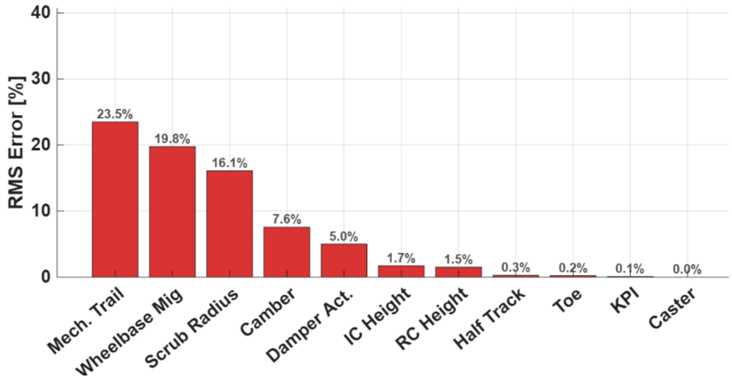

Figure 15: RMS errors for suspension parameters in steer

Figure 16 shows two overlays of different outputs in ARD and in-house solver. Figure 16b depicts the difference in mechanical trail that led to an RMS of 23.5%, whilst Figure 16a depicts the difference in toe that led to an RMS error of 0.2%.

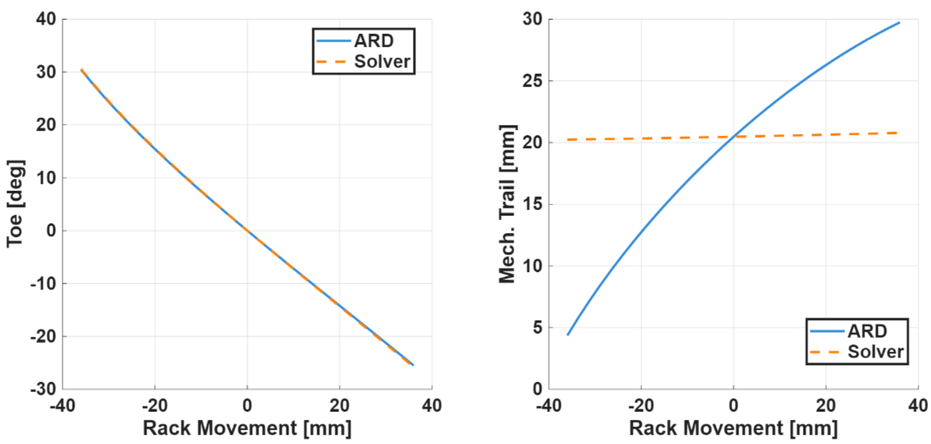

Figure 16: Kinematic solver vs ARD comparison in steering for a) toe, b) mechanical trail

3.3.2. Suspension Development

In collaboration with the IFR team, design targets were set to align with the design strategy of the team's IFR02 car concept in the development of the front suspension. Some of the key changes were in bump steer, roll centre height, scrub radius and camber gain:

The team desired:

- Reduced or eliminated bump steer for better stability.
- Better camber control over the suspension movement.
- Higher roll centre for a lower roll moment and roll angle.
- Lower scrub radius to reduce the steering effort.

The following figures illustrate the kinematic differences made through targeted changes to suspension geometry.

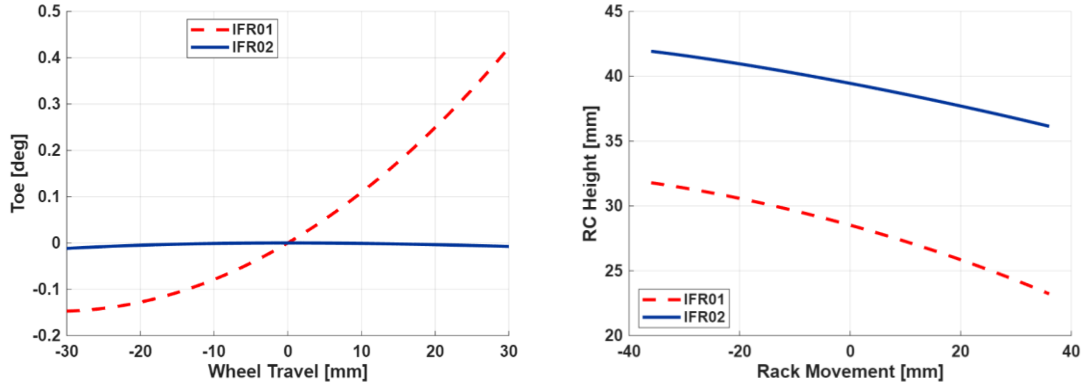

Figure 17: IFR01 vs IFR02 comparison for a) toe in bump, b) roll centre height in steer

.

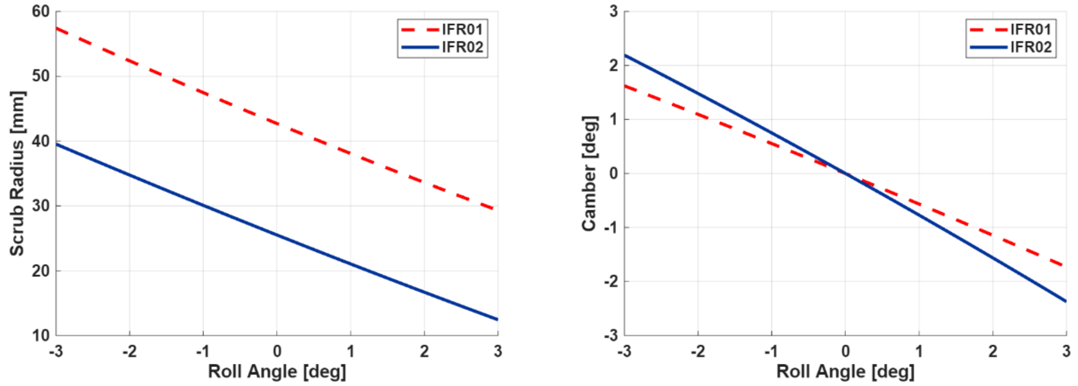

Figure 18: IFR01 vs IFR02 comparison in roll for a) scrub radius, b) camber

3.4. Discussion

3.4.1. Validation

Root mean square error (RMSE) analysis is conducted across the full sweep of values and penalises large deviations, which is important in model validation.

In bump, strong agreement between the kinematic tool and ARD is seen across many channels, seen in Figure 11, and in Figure 12a the near-zero RMS error in camber values is shown. High RMS error is seen in two channels, toe at 30.3% and wheelbase migration at 31.8%, shown in Figure 12b. Despite the 31.8% RMSE in wheelbase migration, the peak absolute error is just 4×10^{-3} mm and highlights the limitations of the RMS analysis where large relative deviations are penalised heavily.

In roll, several key channels are found to have low RMSE, including camber (7.3%), roll centre height (1.6%), shown in Figure 14b, and caster (0.2%). Roll centre height and camber, which only has a peak absolute error of 0.16°, are particularly useful as they are utilised in the later lap simulation work. However, there is significant RMSE in KPI (27.4%), toe (29.9%) and wheelbase migration (29.9%), shown in Figure 14a. When examining Figure 14a, the tool's wheelbase migration remains constant at zero whilst the ARD output varies, leading to a peak absolute error of 2.4 mm, which, combined with the other errors, may point to a difference in how the roll movement is computed between the two tools.

In steer, 8/11 channels have RMSE below 10%, whilst the most significant errors are in mechanical trail (23.5%), wheelbase migration (19.8%) and scrub radius (16.1%). In Figure 16b, the plot of the mechanical trail comparison is shown where the tool output remains close to constant whilst ARD varies significantly. This points to a difference in how this metric is computed, rather than a difference in how the movement is transferred, particularly as the error in toe, i.e. steering angle, is only 0.2% suggesting the steer motion is applied correctly.

Throughout the analyses, there are three parameters that consistently return high RMSE: wheelbase migration, mechanical trail and scrub radius. Mechanical trail and scrub radius are both defined from the projection of KPI and caster distance to the contact patch position, whilst the wheelbase migration is the difference in contact patch location. Given the typically low error in caster and KPI, it can be concluded that the contact patch position, which the wheelbase migration is directly derived from, is the primary reason for the errors seen in these parameters.

Overall, the kinematic analysis tool can be considered validated for suspension design and analysis. A peak RMS error of 31.8% is high but not invalidating as it arises from a derived parameter with diagnosed causes rather than direct resolved geometry, e.g. caster. Camber, roll centre height and toe, key for further design and simulation work, agree closely with the ARD outputs.

3.4.2. Suspension Development

The kinematic analysis tool was utilised to develop the IFR02 front suspension, with the IFR team taking charge of the rear suspension design and collaborating to create a cohesive suspension design. In this process, the targets were to: reduce bump steer, raise the roll centre, improve camber control in roll and reduce scrub radius.

To reduce the bump steer, the tie rod projection was aligned with the instant centre location [4]. Figure 17a shows the improved bump steer, where the peak toe is reduced from 0.4° to -0.05° in maximum bump. This achieves the target set and the same methodology can be applied to further iterations.

To improve camber gain in roll, it was hypothesised that increasing the camber gain would aid the recovery of camber lost in roll and improve lap time. Figure 18b shows the difference of camber gain in roll, with 0.5° of additional camber gain at 3° of roll. To achieve this, a shorter upper wishbone is designed compared to the lower wishbone [1] whilst trying to increase the instant centre height. These changes directly influence the roll centre height, which was raised by increasing the height of the instant centre through this wishbone hardpoints adjustment, whilst keeping the FVSA length sufficient to ensure the correct camber profile. The roll centre comparison is shown in Figure 17b, with a higher roll centre height reducing the roll moment and hence roll angle through hard cornering.

The largest complaint with the IFR01 was the heavy steering, which is a direct function of the scrub radius. Reducing the scrub radius from 43mm to 26mm, as shown in Figure 18a, by offsetting the caster axis leads to a 40% reduction in steering effort since the same rack is reused, improving manoeuvrability around the FS track and reducing driver fatigue in endurance events.

4. Lap time Simulation

4.1. Purpose of Tool

Following on from the kinematic analysis, the ability to determine the dynamic effects of suspension changes on car performance and handling is unknown until the car hits the track. Hence, implementing a new suspension design provides a significant risk and unknown with the level of investment required for introducing parts, particularly for the IFR team who operate under significant cost and resource restraints.

A quasi-static lap simulation (QSLS) is developed to enable analysis of cornering speed, maximum g-force and lap time, utilising the kinematic solvers to provide grip which varies by each individual tyre's camber, slip angle and vertical force.

4.2. Methodology

4.2.1. Track Representation

Utilising telemetry data obtained by the IFR team in the FSUK2025 event, the team were able to generate a csv containing the:

- x, y coordinates,
- k, track curvature (signed to distinguish left/right),
- s, arc length,
- n, number of points.

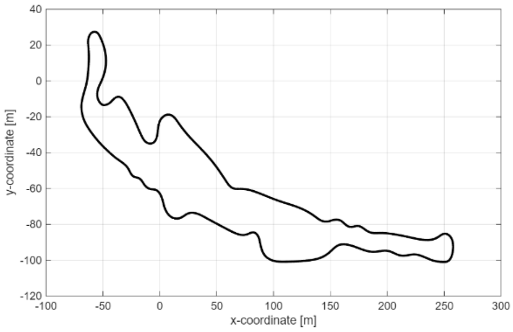

Figure 19: FSUK 2025 Endurance Track Layout

Plotted in Figure 19, the endurance track layout is the best approximation for what the IFR car needs to be optimised to handle. With tight, twisty sections of track and short straight-line bursts, there are conflicting requirements when designing a Formula Student car [2]. Hence, the ability to simulate a lap allows for tailored development to suit an FS competition.

4.2.2. Vehicle Model

A total vehicle mass of 250kg is distributed between the four tyres according to the position of the CoG, as well as the total vehicle wheelbase for appropriate load distribution. This provides the static corner loads, which are supplemented using a simplified aerodynamic model, rolling resistance and load transfer.

4.2.3. Powertrain Model

A simplified powertrain model is utilised, provided by the IFR team, providing a comparable baseline to compare the two simulation packages against one another. Here a 6-speed gearbox, with a 3.5 final reduction, is utilised to provide the tractive force, and hence acceleration in the model at a drivetrain efficiency of 80% due to the chain drive.

Vehicle acceleration is limited by traction, rather than engine power, so doesn’t accurately account for potential wheelspin, particularly in lower grip conditions.

4.2.4. Tyre Model

The IFR Pacejka tyre model is accessed and a 3D lookup table is computed consisting of camber, vertical force and slip angle. At each step of the forwards and backwards passes the solver interpolates between the table values for each parameter. Evaluating at each tyre gives the available car grip, and hence cornering capacity, as opposed to using a single fixed coefficient of friction. A wet grip reduction μ = 0.55-0.70 is determined to simulate the effect of wet conditions, though is rather simplified as there are more dynamic effects of wet running [10].

4.2.5. Simulation Architecture

The simulation utilises the kinematic solver in each step of the forwards and backwards passes, where bump, roll and steer movements are applied to obtain the instantaneous camber, toe and roll centre position for each tyre. Using the load transfer relationships, the vertical tyre force is found and used to generate the lateral tyre grip at each step. Once the lateral force demand is met for corners, the remaining force is utilised to provide longitudinal force for acceleration or braking, hence determining the maximum speed at each step.

4.3. Results

4.3.1. Validation Against ARD

The ARD and in-house simulations were loaded with identical set-ups, with the same torque map, suspension kinematics and vehicle mass, with the only difference in the tyre model implementation. An overlay of the two g-g diagrams is shown in Figure 20, where it is seen that the longitudinal accelerations are similar in magnitude and location, whilst the lateral acceleration of the ARD sim is noticeably less than that of the QSLS as seen with the narrower lateral envelope.

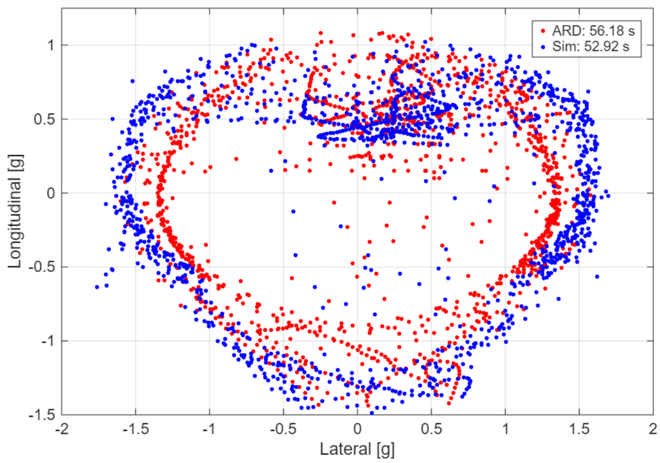

Figure 20: Overlay of g-g plots for ARD and QSLS

In Figure 21a, a speed-distance trace of the ARD and QSLS is shown, where it is seen that the top speed and braking are very comparable, whilst cornering speeds are higher in the QSLS. Figure 21b reinforces this showing the speed is higher for the QSLS compared to the ARD sim where, collectively, these factors lead to a 3 second lap time difference.

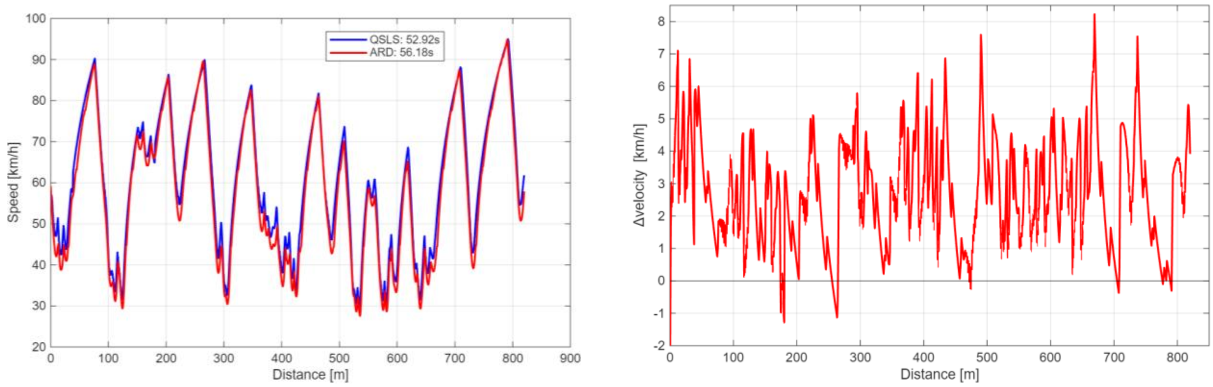

Figure 21: ARD vs QSLS comparison for a) speed-distance trace, b) speed difference

An approximate 15% difference in peak lateral acceleration is shown, so a grip scaling factor of 0.85 was applied to the peak tyre forces. Figure 22 shows the resulting g-g overlay, where the two simulations now agree better in lateral acceleration and is reflected with almost identical lap times.

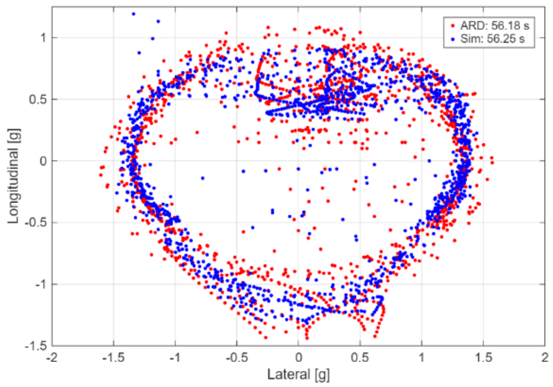

Figure 22: ARD vs grip factor corrected QSLS g-g overlay

In Figure 23a, the speed-distance trace shows closer alignment of the sim speeds throughout the lap. The difference in speed throughout the lap is shown in Figure 23b, where the difference hovers around zero and the lap time difference collapses to practically zero.

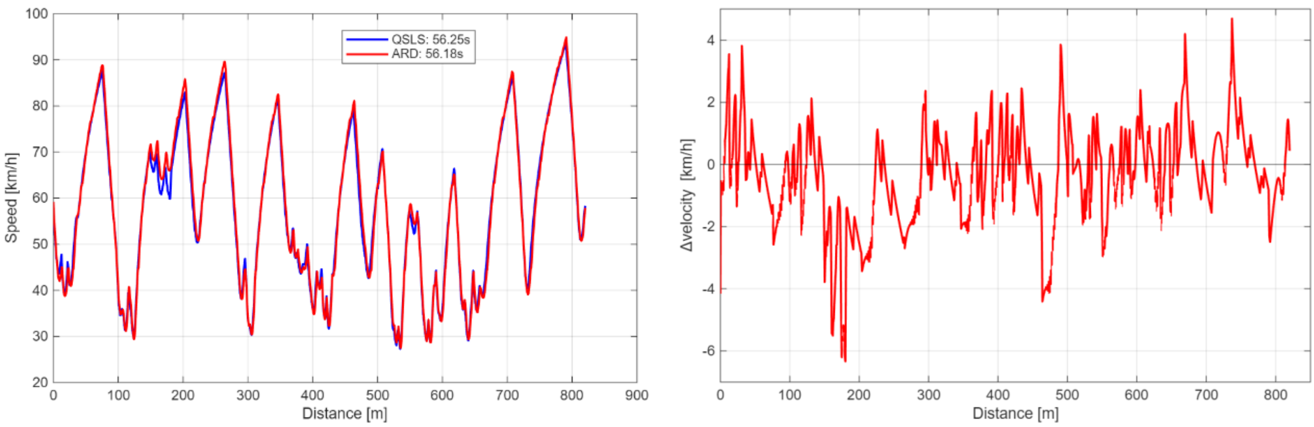

Figure 23: ARD vs grip corrected QSLS comparison for a) speed against distance, b) velocity difference

4.3.2. FSUK Lap Time Comparison

Telemetry from the FSUK2025 event was provided by the IFR team, where the best lap was used to compare against the QSLS lap simulation. A wet grip factor of between μ =0.55-0.70 is used to reduce the available grip and approximate the wet conditions experienced throughout the FSUK2025 endurance event. Figure 24 shows the overlay of the wet telemetry with the QSLS laps with the two grip reduction factors, where it appears that the lap sims and wet telemetry have comparable cornering performance whilst the top speed of the wet telemetry was significantly lower than either lap sim.

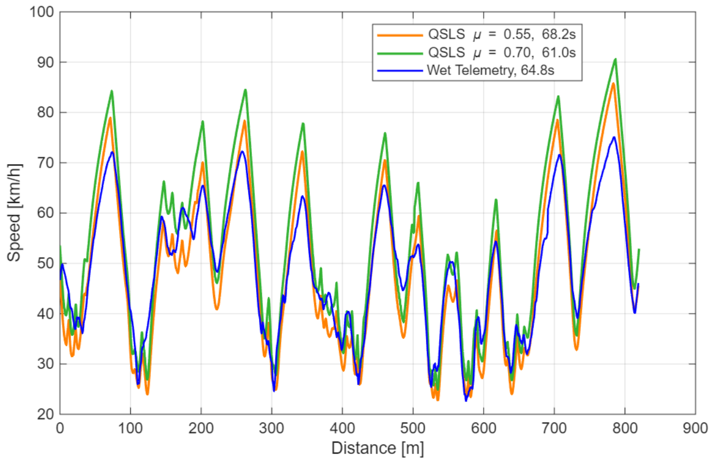

Figure 24: Speed-distance trace comparing FSUK fastest lap and QSLS

To further quantify the difference, a μ value of 0.625 is chosen as it provided a 0.4s lap time difference to that of the telemetry. Figure 25a shows the subsequent speed trace, where the top speed of the simulation is significantly greater than the telemetry whilst the cornering speeds are comparable. Figure 25b shows the speed delta between the sim and telemetry, with broad agreement in the cornering performance.

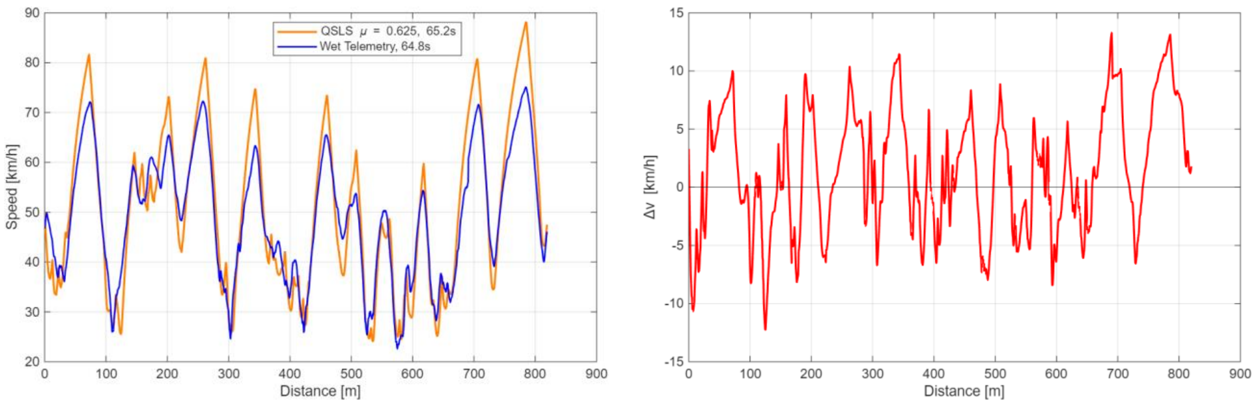

Figure 25: Wet telemetry vs lap sim data for a) speed-distance trace, b) speed delta plot

4.3.3. Sensitivity Study

The first sensitivity study was in the variation of spring stiffness between 125-250 lb/in, finding 0.5s of improvement when using a front/rear configuration of 250/175 lb/in compared to 125/250 lb/in.

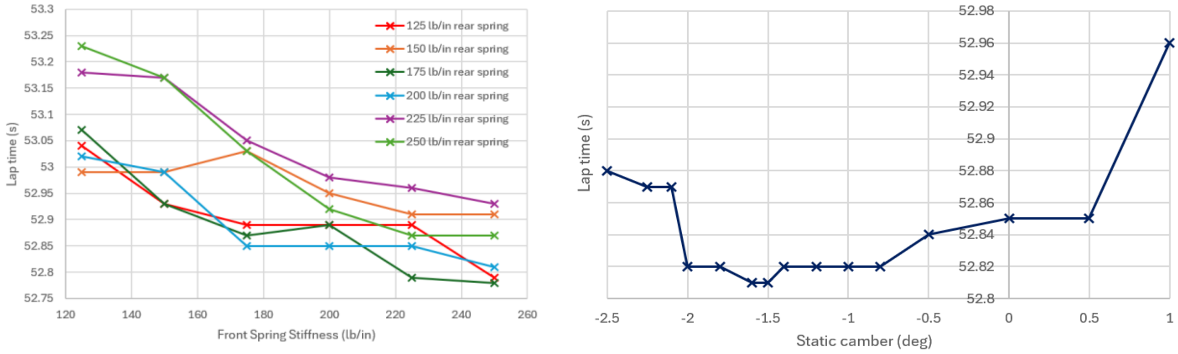

Figure 26: Sensitivity study a) Spring stiffness, b) Static camber

The second sensitivity study was conducted by varying the front static camber and analysing the lap time difference. Plots of the dynamic camber through the lap are shown in Figure 27, where they are compared to the peak-grip camber of -0.4°.

4.4. Discussion

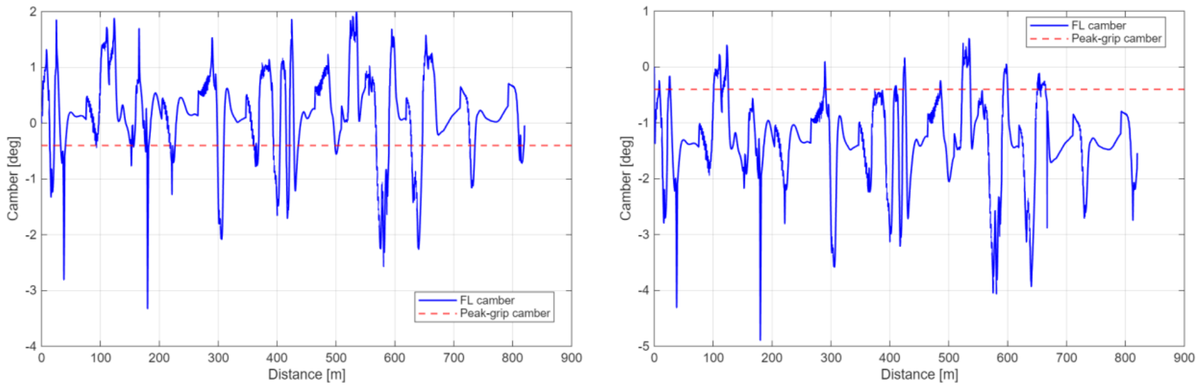

Figure 27: Dynamic front left camber comparison with static camber: a) 0 deg static camber, b) -1.5 deg static camber

4.4.1. ARD validation

The ARD sim and QSLS tool were configured identically, including torque map, suspension geometry and vehicle mass, with the only known difference in the tyre model due to a different implementation method in ARD as opposed to a direct lookup table from the QSLS.

Initially, there is a ~3 second lap time difference between the two simulations, with the QSLS giving 52.92s and ARD 56.18s. In Figure 20, the QSLS g-g plot is wider than the ARD plot, suggesting the QSLS predicts a higher cornering capacity than the ARD sim, which can also be seen with the higher minimum corner speeds in Figure 21a. The longitudinal performance of the two simulations is similar, with the g-g height being comparable and the top speed and braking profiles remaining close to identical. These factors suggest that the tyre forces generated are optimistic in comparison to ARD, resulting in a ~15% difference between peak lateral g of the two simulations.

To further localise whether this was the cause, a 15% reduction in peak lateral tyre forces was used as this was the approximate percentage difference in peak lateral acceleration (1.6g vs 1.4g). Figure 22 shows the g-g diagrams overlapping, with the speed trace also very comparable in straight-line and cornering speed, leading to the lap time difference falling to close to zero. Essentially, this confirms that the primary difference between the two simulations is how tyre forces are computed and generated, with a 15% difference in the peak lateral forces generated between the two whilst the remainder of the simulation framework is comparable, with speed difference between the two averaging at ±2km/h over the lap.

4.4.2. Telemetry validation

The fastest lap from the IFR team was obtained from the FSUK2025 telemetry and used to compare against the QSLS. The data was collected in wet conditions, meaning that the same tyre model could not be used so a grip reduction factor of 0.55-0.70 was utilised.

When μ=0.625, the lap time difference between the QSLS and telemetry is 0.4s. The speed trace also indicates that the two laps have very comparable cornering speeds, with variations in which is quicker in various corners. This is likely due to the driver being able to take a better racing line and hence can carry more speed through the corners. However, there is a clear divergence in the top speed and acceleration, where the QSLS overestimates the speed by around 10km/h at the end of straight. The top speed discrepancy is likely due to overoptimistic powertrain modelling by the IFR team or an engine issue at the event.

4.4.3. Sensitivity Study

The two parameters analysed in the sensitivity study were front static camber and spring stiffness, key suspension set-up parameters.

The spring stiffness analysis indicated a 0.5s lap time improvement when employing 250/175 lb/in front-rear spring configuration, when compared to a 125/250 configuration. This is a reasonable lap time gain and aligns closely to the chosen IFR spring stiffness utilised of 250/200 lb/in.

The lap time gain in the camber analysis is more modest, at only 0.15s difference between -1.5° and +1° of static camber. Positive camber is detrimental to tyre performance, and hence the effect of static negative camber is expected to be more pronounced. Despite this, without on track testing of these parameters a conclusion on the sensitivity of the tool to camber changes cannot be drawn.

4.5. Limitations and Recommendations for future work

A QSLS does not model some key concepts such as yaw and damping, which means that there are some vehicle dynamics effects that aren't modelled. These effects would inevitably impact performance, so transition to a dynamic lap simulation would enable a more comprehensive outlook on vehicle performance.

Validating the QSLS with dry on-track running would be particularly beneficial, as it enables a direct comparison to the vehicle performance using the exact tyres without a scaling factor. Further to this, the model can then be adapted to provide further correlation around different configurations imitating a typical FS track.

5. Design Improvements

Now that the lap simulation tool has been validated, it can be used to analyse the IFR02 concept and implement kinematic changes, using the tool, to further improve the lap time.

5.1. IFR02 Concept

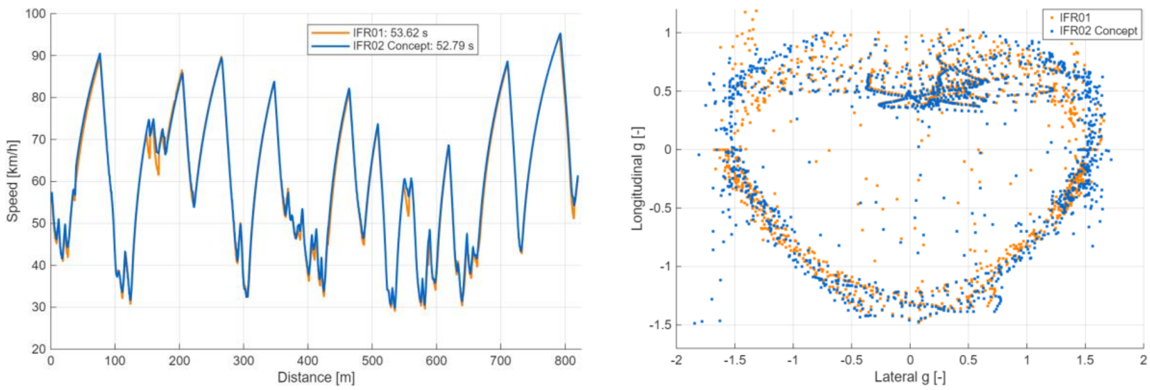

Figure 28: IFR01 vs IFR02 Concept comparison in a) speed-distance trace, b) g-g diagram

The IFR02 concept was generated in Section 3, purely through kinematic analysis, and is seen to provide a 0.83 second lap time improvement compared to the IFR01, Figure 28.

Analysis of the output channels and further discussions with the IFR team formed the basis for further design changes to be made.

5.2. Kinematic Changes

Through analysis of the camber channel for the IFR02 Concept QSLS, it was seen that the camber throughout the lap was overcompensating for the amount of roll the car was experiencing. Hence, the camber gain was reduced to ensure that the camber of the tyre remained in the optimum camber angle for longer.

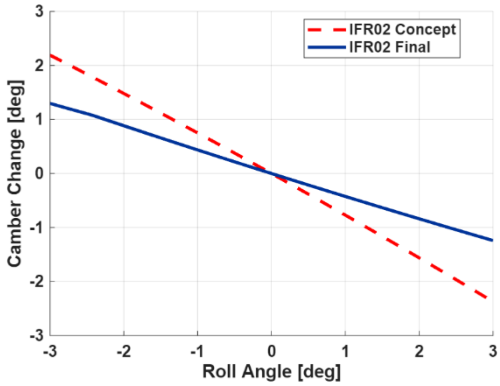

Figure 29: Revised camber in roll plot

Together with the IFR team, the decision was made to reduce the track from 1250mm to 1180mm as well as further reduce the scrub radius and increase roll centre height.

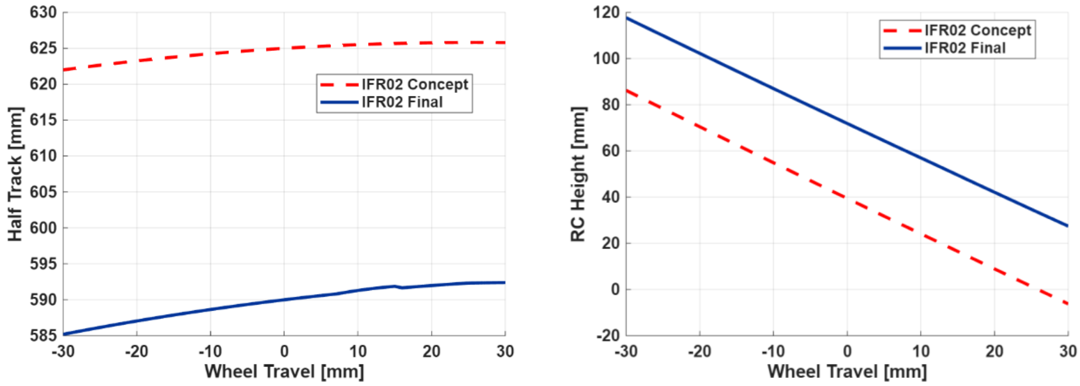

Figure 30: Revised a) half track in bump, b) roll centre height in bump

5.3. IFR02 Final Design

Following the design changes, the speed-distance trace and g-g diagram are illustrated below, where a further 0.62s lap time improvement is found.

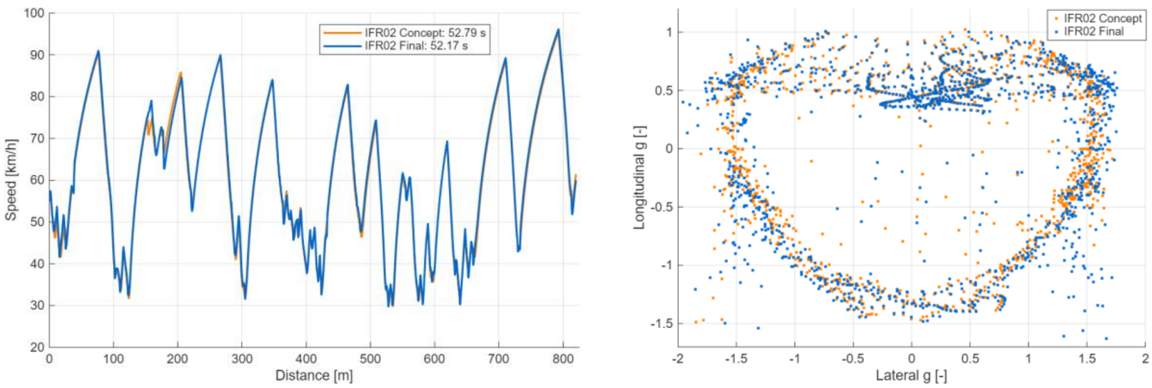

Figure 31: Comparison of Concept vs Final a) speed-distance trace, b) g-g diagram

To provide a better visualisation of the changes and their effect on vehicle performance, the front-left dynamic camber and vehicle chassis roll are shown in Figure 32. Here, peak chassis roll is reduced and camber is closer to the peak-grip camber.

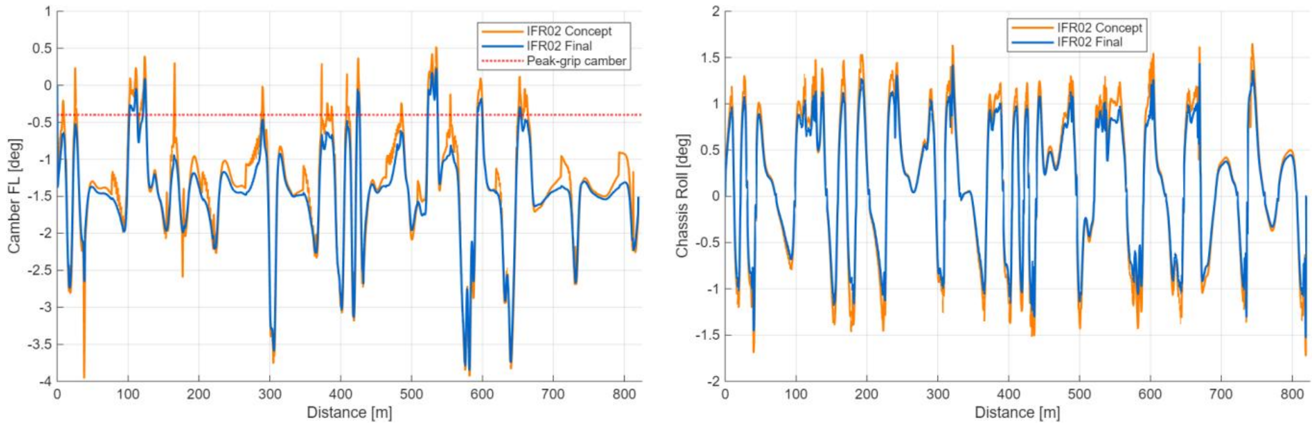

Figure 32: Concept vs Final comparison plot for a) front left dynamic camber, b) chassis roll

Figure 33 illustrates the lap time difference throughout the design process.

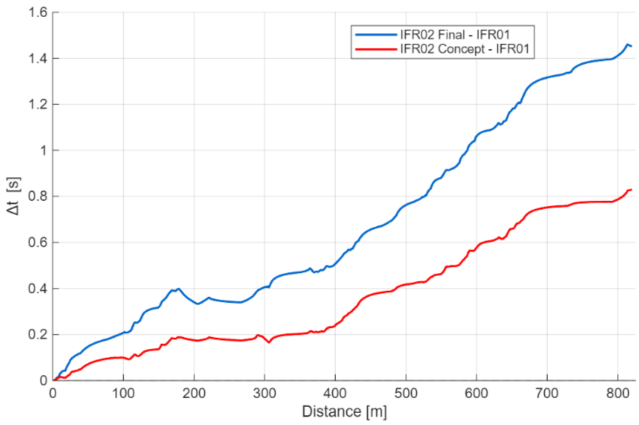

Figure 33: Lap time improvement in the design process

5.4. Discussion

The camber channel of the Concept sim was analysed and it was found that peak camber values throughout the lap were overshooting the -0.4° camber value which provides peak grip. Despite this, a 0.83s improvement was still found, so further refinement would enable further lap time improvements.

In discussion with the IFR team, the front track was reduced from 1250mm to 1180 mm, which has the effect of increasing the lateral load transfer and induces a greater roll moment on the chassis and hence roll angle. To combat the increased roll angle, the roll centre height was increased to reduce the roll moment and hence roll angle that the car experiences. Camber gain in roll was also reduced, which has the effect of reducing the peak camber obtained, a decision taken after iterative analysis using various camber gain profiles, to provide the optimal vehicle performance.

The result of these changes led to a further 0.62s lap time gain over the IFR02 Concept and a total 1.45s improvement over the IFR01 design, worth 4 places in the FSUK2025 sprint event [11] for the IFR team, potentially increasing the opportunity for sponsorship and publicity.

6. Conclusion

This project set out to provide accessible, in-house tools to facilitate iterative suspension design, with the ability to quantify the effect of geometrical changes on kinematics and vehicle performance. Two MATLAB tools were created, validated and then utilised to generate an IFR02 front suspension design.

The first tool was a kinematic analysis tool, validated against ARD across all suspension movements, with a peak RMS error of 31.8%. The reason for errors is traced primarily to the way that the contact patch is computed between the two leading to errors in parameters derived from the contact patch, though the large majority of parameter channels have low RMS errors. The kinematic analysis tool was utilised to create an IFR02 Concept, fulfilling the targets set by the IFR team.

The second tool was a Quasi-Static Lap Simulation tool, where a 15% error in peak lateral tyre force compared to ARD was found, which was resolved with a grip reduction factor to correct the grip difference between the two. Validation was also undertaken against wet telemetry data from the IFR team obtained during the FSUK2025 event. To provide a comparative analysis, a wet grip scale factor of 0.625 was utilised to give a lap time difference of 0.4s. The cornering performance was comparable and inspired confidence in the output, though the QSLS overshot the straight-line speed, which indicates optimistic powertrain modelling or an engine issue at the event.

The QSLS was used to analyse the performance of the IFR02 Concept before implementing iterative kinematic improvements to generate a quicker final design. Whilst the IFR02 Concept was 0.83s faster than the IFR01, a further 0.62s lap time improvement was found with kinematic refinements. Overall, a lap time gain of 1.45s for IFR02 Final Design over the IFR01 was achieved, worth a four-place position improvement in the FSUK2025 sprint event.

In conclusion, this project leaves the IFR team with two in-house tools which can be used for comprehensive suspension design. With further development, the QSLS can be adapted to provide dynamic lap simulations which would enable more comprehensive analysis of the dynamic effects of the vehicle.

7. Declaration of AI Use

AI assisted writing, using Claude, was used in the writing of this report, primarily to improve writing style, reduce word count and ensure all relevant content is discussed. Sections of the text which lacked the necessary flow were inputted into the AI and given specific prompts to which the AI suggested revisions to achieve the targets in the prompts. All technical content was first drafted by me, with AI providing reminders of any missed discussion points, structural and writing recommendations.

AI was utilised to debug code throughout this project and streamline a lot of the heavy coding requirements when plotting output and comparison parameters. One example where AI assisted coding was used was the lap simulation overlays, which saved significant time in writing sections of code to generate the necessary plots, which I specified to the AI alongside a baseline code.

8. References

[1] D. Seward, *Race Car Design*. 2014.

[2] M. Suli, “Single Seater Race Car Optimisation”, ME3 Literature Review Project, 2024.

[3] M. W. Arshad, S. Lodi, and D. Q. Liu, “Double Wishbone Suspension: A Computational Framework for Parametric 3D Kinematic Modeling and Simulation Using Mathematica,” *Technologies (Basel).*, vol. 13, no. 8, Aug. 2025, doi: 10.3390/technologies13080332.

[4] Milliken and Milliken, *Race Car Vehicle Dynamics*. 1995.

[5] S. I. Valencia Arboleda, “Design of the suspension system for a FSAE race car,” 2017.

[6] B. Siegler, A. Deakin, and D. Crolla, “Lap Time Simulation: Comparison of Steady State, Quasi- Static and Transient Racing Car Cornering Strategies,” Nov. 2000. doi: 10.4271/2000-01-3563.

[7] D. L. Brayshaw and M. F. Harrison, “A quasi steady state approach to race car lap simulation in order to understand the effects of racing line and centre of gravity location,” *Proceedings of the Institution of Mechanical Engineers, Part D: Journal of Automobile Engineering*, vol. 219, no. 6, pp. 725–739, Jun. 2005, doi: 10.1243/095440705X11211.

[8] C. Patton, “Development of Vehicle Dynamics Tools for Motorsports,” 2013.

[9] H. B. Pacejka and E. Bakker, “The Magic Formula Tyre Model,” in *Tyre Models for Vehicle Dynamics Analysis*, London: CRC Press, 2026, pp. 1–18. doi: 10.1201/9781003760634-1.

[10] J. Y. Wong, *Theory of Ground Vehicles*. 2022.

[11] Institution of Mechanical Engineers, “Formula Student 2025 — Sprint Event Results.”

[12] OptimumG, “OptimumLap v1.4: Vehicle Dynamics Simulation,” 2015.

[13] R. P. Costa and R. Bortolussi, “Lap Time Simulation of Formula SAE Vehicle With Quasi-steady State Model,” Oct. 2016. doi: 10.4271/2016-36-0164.